Robust Control of a Quadrotor in the Presence of Actuators' Failure

Yasser Mousalou
Department of Electrical Engineering, Ahar Branch, Islamic Azad University,Ahar, iran
Email: y_mousalou@yahoo.com

Abstract

Today, robots and unmanned aerial vehicles are being used extensively in modern societies. Due to a wide range of applications, it has attracted much attention among scientists over the past decades. This paper deals with the problem of the stability of a four-rotor flying robot called quadrotor, which is an under-actuated system, in the presence of operator or sensor failures. The dynamical model of quadrotor is expressed in terms of different physical phenomena by the Newton-Euler method. Subsequently, a back stepping control approach has been developed, considering actuator and sensor failures. The stability analysis based on the Lyapanov method shows that the designed control strategy maintains the stability of quadrotor closed loop dynamics even in the presence of failures. The simulations of the control system indicate that the proposed control strategy is capable of maintaining performance and maintains system stability in the event of a failure of the operator or sensor.

Keywords: robot, quadrotor, under-actuated, back-stepping Controller, actuator and sensor failure.

1. Introduction

Today unmanned flying objects are utilized in spy aircrafts [1], search and rescue operations in dangerous and exotic areas [2], fire rescue operations [3], controlling power plants and nuclear reactors [4], mapping [5], border patrol functions [6], visiting oil and gas transportation lines [1], navy operations [7], and controlling urban traffic [1], due to the lack of use a human force as a pilot. Vertical flyers are more popular because of their floating capability in the air and also high maneuvering capabilities. Vertical flying vehicles are divided into some categories as: normal helicopters, coaxial helicopters, and different rotators with different structures. From among them, quadrotors or quadcopters are deemed highly important due to their simple structures and lack of need to complicated mechanical connection points and they can be forced to have any desired movement through changing propeller rotation.

In 1907 Berguit Brother and Professor Charles Richet created a vertical flying aircraft of Gyroplane [8]. Ettine Oemichen was another engineer who thought of an aircraft with rotating wings in 1920 [2 PRD]. In year 1921, Dr. Georgede Bothezat and Ivan Jerome signed a contract to develop one of these aircrafts for aerial force of the United States [9]. Since the construction and

development of sensors and designing control systems were not possible in that era, it was practically impossible to design automated aircraft.

Unmanned aircrafts are favored more because of their simpler structures, reasonable costs, doing more specialized operations, lower noises, and lack of being recognized by radars in spy operations. But the most important advantage of such aircrafts is that they can carry out difficult and dangerous operations without endangering the life of a human being as a pilot. The major advantage of using quadrotors compared to other aircrafts with fixed wings is that they have a high capability in flights in low heights, closed environments and at times there is a need for high maneuver capability compared to fixed wing aircrafts. The capability of vertical flight enables them to take off and land in any location. Therefore, quadrotors are designed and produced in different sizes and with different facilities.

In reference [10], Altung and et al tried to extract dynamic equations of quadrotors for the first time using Newton-Euler method. In reference [11], Bouabdallah and et al designed OS4 micro-quadrotor including dynamic design, dynamic modeling, and angels' measurement and control.

Pounds and et al were studying on a design of a 4 rotors helicopter in National University of Australia which ended in designing an aircraft called XII-4FlyerMark [52]. Mokhtari and et al merged a resistant linear feedback with a linear GH∞ control to control a nonlinear quadrotor.

Huffman and et al [14], were trying to resolve some problems that could create chaos in floating flight system aircrafts. In [15], the adaptive sliding mode controller was developed for the consistency of the behavior and to trace the route. In reference [16] a quadrotor under stimulation of a parametric indefiniteness has been investigated. A back-stepping controller has been used to design a nonlinear controller. In [17] an integration of the two methods of nonlinear back-stepping and sliding mode control has been benefited to control the quadrotor. In [18], the hybrid back-stepping and Frenet-Serret theory for the consistency of the quadrotor state have been utilized. A new neural-comparative controller has been designed to achieve consistency of the quadrotor and to fight against the chaos [19].

In [20], tolerant fault estimation design has been proposed to control the quadrotor. First the comparative Tao observer has been used to estimate the actuators' faults of different states of the quadrotor and to calculate the set of fault residuals. Reference [21] deals with designing a self-reforming controller based on sliding mode comparative control method for the quadrotor with actuators' fault. A fault tolerant controller [22] based on temporary efficiency index has been introduced to control the quadrotor with actuators' fault. Reference [23] has dealt with designing, analysis, and implementation of a fault tolerant resistant comparative controller to control the state and height of the quadrotor without requiring the use of a fault recognition mechanism. In reference [24], a sliding mode comparative fuzzy controller has been proposed to adjust the great faults of the actuators and to hold the quadrotors consistent.

In this research, first a quadrotor modeling has been done using a Newton-Euler method. Then, a resistant control method based on a back-stepping has been proposed to control and stabilize quadrotor flights in the presence of actuators' and sensors' faults.

2. Quadrotor modeling

Quadrotors could neutralize the forces of the moments created through utilizing 4 motors and isolated blades and reverse binary rotations of these motors and also supply the required pressure difference to create trust forces [25].

Every propeller creates a force and a moment proportionate with the square root of its velocity. The direction of the produced forces is upwards and the direction of moments is counter propeller rotations. Figure 1 represents a simple structure of a quadrotor. The quadrotor body is like a cross whose useful load (sensors, controllers, central processor, camera, ...) lies in its center. A motor and an electric motor with a direct flow without step-backing have been installed on any ending which has a light propeller mounted on it. The controlling input is done solely through changing the motors' rotary distance. The couples of cross propellers are installed across from each other on an arm and rotates counter to the other one.

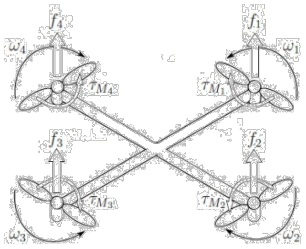

Fig.1. The simple quadrotor structure

Quadrotor has 6 degree of freedom and to control these 6 degrees of freedom, 4 input controls (a 4 motors controller) have been installed and thus the system is under the stimulation. Therefore, some are not independent of each other and in some cases several movements occur concurrently. For example, when the quadrotor moves forwards (movement along axis x), the aircraft rotates along with axis y (pitch).

To compose dynamic equations we can not consider all parameters involved in a phenomenon, because natural systems and specifically the flight systems are complicated and different factors affect their dynamicity and movements. Therefore, to simplify the process, we do not consider some of the parameters. For the quadrotor and to resolve the problems related, we will consider the followings:

- The quadrotor system is rigid.
- Its geometrical and mass structure is symmetrical.
- The mass center and the local coordinates' center are congruent and are located in the center of the object.
- The upward force and the resistant force of the rotation of the propellers are proportionate with the square angle velocity.

To calculate the dynamic and cinematic equations, first the two reference coordinates are introduced. The body coordinates (local) rigidly stock onto the object and the absolute coordinates (global or inertia) are based on figure 2 and we have the followings for both sets: B(x,y,z) and E(X,Y,Z).

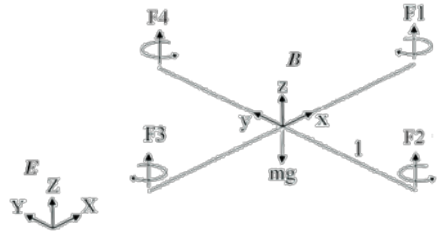

Fig.2.The local and absolute coordinates determined for the quadrotor

As we define the following variables, the descriptive equations can calculate the results as follows:

$\zeta = (X, Y, Z)$

Position vector in absolute coordinates (inertia)

$V = (u, v, w)$

The linear transformation velocity vector proportionate to the body

$\omega = (p, q, r)$

The rate of Euler angles' changes proportionate to the local (body) coordinates

$\eta = (\phi, \theta, \psi)$

Euler angles proportionate to the absolute (inertia) coordinates

The relationship between velocity vector (v, ω) and the derivations of the absolute coordinates' vector and Euler angles $(\dot{\zeta}, \dot{\eta})$ are as follows:

$$\begin{cases} \dot{\zeta} = R_t v \\ \dot{\eta} = R_r \omega \end{cases} \tag{1}$$

Where, the matrixes R_t and R_r represent linear velocity transformation matrix and angle velocity between the two local and absolute coordinates' sets, respectively.

$$R_t = \begin{bmatrix} c\psi c\theta & c\psi s\theta s\phi - s\psi c\phi & c\psi s\theta c\phi + s\psi c\phi \\ s\psi c\phi & s\psi s\theta s\phi + c\psi c\phi & s\psi s\theta c\phi - c\psi s\phi \\ -s\theta & c\theta s\phi & c\theta c\phi \end{bmatrix} \tag{2}$$

$$R_r = T = \begin{bmatrix} 1 & 0 & -s\theta \\ 0 & c\phi & s\phi c\theta \\ 0 & -s\phi & c\phi s\theta \end{bmatrix} \tag{3}$$

$$R_t^{-1} = R_t^T \tag{4}$$

The matrixes (2) and (3) represent the trigonometrically equations for sinus and cosines.

The dynamic of the rigid object affected by the external forces on the mass center based on Newton-Euler formula expressed in body set is as follow

$$\begin{bmatrix} m \times I_{3\times3} & 0_{3\times3} \\ 0_{3\times3} & I \end{bmatrix} \begin{bmatrix} \dot{V} \\ \dot{\omega} \end{bmatrix} + \begin{bmatrix} \omega \times (mV) \\ \omega \times (I\omega) \end{bmatrix} = \begin{bmatrix} F \\ \tau \end{bmatrix} \tag{5}$$

Where, F and τ represent the external forces and moments enforced on the aircraft, m represents total object mass and ω represents the angle velocity between the two sets of body

coordinates and absolute coordinates (or inertia). In second equation, $= \begin{bmatrix} I_{xx} & -I_{xy} & -I_{xz} \\ -I_{xy} & I_{yy} & -I_{yz} \\ -I_{zx} & -I_{zy} & I_{zz} \end{bmatrix}$, is the inertia matrix and it is fixed. Considering a symmetrical structure for the quadrotor, this matrix can be written as the following form. Thus, we will have:

$$I = \begin{bmatrix} I_{xx} & 0 & 0 \\ 0 & I_{yy} & 0 \\ 0 & 0 & I_{zz} \end{bmatrix} \tag{6}$$

To simplify the control rules of Euler angles and quadrotor position, we can transfer the equations above using equations (2), (3), and (7) into the earth coordinates set as follows:

$$\dot{R} = RS(\Omega) \tag{7}$$

In equation (7), $S(\Omega)$ refers to:

$$S(\Omega) = \begin{pmatrix} 0 & -\Omega_3 & \Omega_2 \\ \Omega_3 & 0 & -\Omega_1 \\ \Omega_2 & \Omega_1 & 0 \end{pmatrix} \tag{8}$$

Thus, the transformation movement equations will be achieved as shown in (9)

$$m\ddot{\xi} = F_f + F_t + F_g \tag{9}$$

In rotary movement equations, if the movement angle is small, the transformation matrix T will be equal to unit 1 and the angle changes in body coordinates will be equal with Euler angles' derivation. This approximation along with a good deal of precision requires the use of a complete model in devising control rules:

$$\dot{\eta} \cong \omega \rightarrow\rightarrow\rightarrow \ddot{\eta} \cong \dot{\omega} \tag{10}$$

Therefore, the dynamic equation of the rotary system will be as follows:

$$I\dot{\omega} = -\omega \times I\omega + \Gamma_f - \Gamma_a - \Gamma_g \tag{11}$$

In equations (9) and (11):

F_f is the equilibrium point of the forces produced by the four rotors:

$$F_f = \begin{pmatrix} C\phi C\psi S\theta + S\phi S\psi \\ C\phi S\theta S\psi + S\phi S\phi \\ C\phi C\theta \end{pmatrix} \sum_{i=1}^{4} F_i \tag{12}$$

$$F_i = b\omega_i^2 \tag{13}$$

B is the fixed amount of ascending (trust) and ω_i is the angle velocity of the ith rotor. $F_f = [F_{tx}, F_{ty}, F_{tz}]^T$ is the equilibrium of the pulling forces along with the coordinates of (x,y,z):

$$F_t = \begin{pmatrix} -K_{ftx} & 0 & 0 \\ 0 & -K_{fty} & 0 \\ 0 & 0 & -K_{ftz} \end{pmatrix} \dot{\xi} \tag{14}$$

Where, K_{ftx} , K_{fty}, K_{ftz} are positive pull coefficients.

F_g is the gravity force and is represented as follows:

$$F_g = [0 \quad 0 \quad -mg]^T \tag{15}$$

Γ_f is found when it is created by the fixed frame of the quadrotor body. As:

$$\Gamma_f = \begin{pmatrix} l(F_3 - F_1) \\ l(F_4 - F_2) \\ d(\omega_1^2 - \omega_2^2 + \omega_3^2 - \omega_4^2) \end{pmatrix} \tag{16}$$

L refers to the distance between the canonical point and propeller rotation center and d is the fixed amount of pulling.

Γ_a is the result of aerodynamic momentum:

$$\Gamma_a = \begin{pmatrix} K_{fax} & 0 & 0 \\ 0 & K_{fay} & 0 \\ 0 & 0 & K_{faz} \end{pmatrix} \omega^2 \tag{17}$$

Where, K_{fax} , K_{fay}, K_{faz} are known as aerodynamic friction coefficients.

Γ_g is the resultant of the moments due to stereoscopic effects:

$$\Gamma_g = \sum_{i=1}^{4} \omega \wedge J_r \begin{bmatrix} 0 \\ 0 \\ (-1)^{i+1}\omega_i \end{bmatrix} \tag{18}$$

J_r is the rotor inertia.

The complete dynamic model dominating the quadrotor, considering the parameters above, is as follows:

$$\begin{aligned} \ddot{\phi} &= \frac{1}{I_{xx}}[(I_{yy} - I_{zz})\dot{\theta}\dot{\psi} - J_r\bar{\Omega}_r\dot{\theta} - K_{fax}\dot{\phi}^2 + lu_2] \\ \ddot{\theta} &= \frac{1}{I_{yy}}[(I_{zz} - I_{xx})\dot{\phi}\dot{\psi} + J_r\bar{\Omega}_r\dot{\phi} - K_{fay}\dot{\theta}^2 + lu_3] \\ \ddot{\psi} &= \frac{1}{I_{zz}}[(I_{xx} - I_{yy})\dot{\theta}\dot{\phi} - K_{faz}\dot{\psi}^2 + u_4] \\ \ddot{x} &= \frac{1}{m}[(C\phi C\psi S\theta + S\phi S\psi)u_1 - K_{ftx}\dot{x}] \\ \ddot{y} &= \frac{1}{m}[(C\phi S\theta S\psi - S\phi C\psi)u_1 - K_{fty}\dot{y}] \\ \ddot{z} &= \frac{1}{m}[(C\phi C\theta)u_1 - K_{ftz}\dot{z}] - g \end{aligned} \tag{19}$$

Presupposing the sub-equations for 19 we can have:

$$\begin{cases} u_x = (C\phi C\psi S\theta + S\phi S\psi) \\ u_y = (C\phi S\theta S\psi - S\phi S\psi) \end{cases} \tag{20}$$

Where,

$$\begin{aligned}
\ddot{\phi} &= [\left(\frac{I_{yy}-I_{xx}}{I_{xx}}\right)\dot{\theta}\dot{\psi} - \frac{J_r}{I_{xx}}\bar{\Omega}_r\dot{\theta} - \frac{K_{fax}}{I_x x}\dot{\phi}^2 + \frac{l}{I_{xx}}u_2] \\
\ddot{\theta} &= [\left(\frac{I_{zz}-I_{xx}}{I_{yy}}\right)\dot{\phi}\dot{\psi} + \frac{J_r}{I_{yy}}\bar{\Omega}_r\dot{\phi} - \frac{K_{fay}}{I_{yy}}\dot{\theta}^2 + \frac{l}{I_y}u_3] \\
\ddot{\psi} &= [\left(\frac{I_{xx}-I_{yy}}{I_{zz}}\right)\dot{\theta}\dot{\phi} - \frac{K_{faz}}{I_{zz}}\dot{\psi}^2 + \frac{1}{I_{zz}}u_4] \\
\ddot{x} &= [\frac{1}{m}u_x u_1 - \frac{K_{ftx}}{m}\dot{x}] \\
\ddot{y} &= [\frac{1}{m}u_y u_1 - \frac{K_{fty}}{m}\dot{y}] \\
\ddot{z} &= \left[\left(\frac{C\phi C\theta}{m}\right)u_1 - \frac{K_{ftz}}{m}\dot{z}\right] - g
\end{aligned} \tag{21}$$

In which u_1, u_2, u_3, and u_4 are system control signals regarding the angular velocity of the 4 rotors and are as follows:

$$\begin{bmatrix} u_1 \\ u_2 \\ u_3 \\ u_4 \end{bmatrix} = \begin{pmatrix} b & b & b & b \\ 0 & -lb & 0 & lb \\ -lb & -b & -lb & b \\ d & -d & d & -d \end{pmatrix} \begin{bmatrix} \omega_1^2 \\ \omega_2^2 \\ \omega_3^2 \\ \omega_4^2 \end{bmatrix} \tag{22}$$

$$\bar{\Omega}_r = \omega_1 - \omega_2 + \omega_3 - \omega_4 \tag{23}$$

$$\begin{cases} J_r\dot{\omega}_i = \tau_i - Q_i\,, & i\epsilon\{1,2,3,4\} \\ Q_i = d\omega_i^2 \end{cases} \tag{24}$$

Q_i is the mpment of the produced reactive in free air through a drag rotor of ith in τ_i input moments. The control rule for the input moment is as follows

$$\tau_i = Q_i + J_r\dot{\omega}_{d,i} - k_i\tilde{\omega}_i \tag{25}$$

$$\tau_i = Q_i + J_r\dot{\omega}_{d,i} - k_i\tilde{\omega}_i \tag{26}$$

$$V_m = \frac{R_a}{k_m k_g}\tau_i + k_m k_g \omega_i, i\epsilon\{1,2,3,4\} \tag{27}$$

Where, $k_i\epsilon\{1,..,4\}$ are 4 positive parameters, $\dot{\omega}_{d,i}\epsilon\{1,..,4\}$ is the optimal speeds of each of the rotors and we have $\tilde{\omega}_i = \omega_i - \dot{\omega}_{d,i}$

$\dot{\tilde{\omega}}_i$ represents index coincidence of ω_i and $\omega_{d,i}$ and tries to lead for the congreuence of body frame moments towards the desired amounts that will lead to a consistent quadrotor status. D.C. motors are controled through control voltages. The inductance of the motors is low. R_a, k_m, k_g are internal motor resistance, fixed motor moment, and gearbox coefficient, respectively. V_m is motor voltage and J_T is inertia.

Quadrotor control strategy with actuators faults

The complete model achieved through the addition of actuator faults and sensr faults in the model can be represented as follows:

$$\begin{cases} \dot{x}(t) = \delta(x,t) + g(x,t)\big(u(t) + f_a(t)\big) \\ y(t) = h(x,t) + f_s(t) \end{cases} \tag{28}$$

Where, $x(t) \in \Re^n$ is the system status vector, $y(t) \in \Re^p$ is the measured output vector, $u(t) \in \Re^m$ is the input controlling vector, $f_a(t) \in \Re^{q_a}$ is the resultant vector of the faults related to quadrotor actuators, and $f_s(t)\varepsilon\, R^{qs}$ is the resultant vector of sensor faults. We have:

$$\begin{aligned} x &= [x_1, \dots, x_{12}]^T \\ &= [\phi, \dot{\phi}, \theta, \dot{\theta}, \psi, \dot{\psi}, x, \dot{x}, y, \dot{y}, z, \dot{z}]^T \end{aligned} \tag{29}$$

Considering actuator faults and velocity sensor faults we have:

$$\begin{aligned}
\dot{x}_1 &= x_2 \\
\dot{x}_2 &= a_1x_4x_6 + a_2x_2^2 + a_3\bar{\Omega}_r x_4 + b_1(u_2 + f_{a1}) \\
\dot{x}_3 &= x_4 \\
\dot{x}_4 &= a_4x_2x_6 + a_5x_4^2 + a_6\bar{\Omega}_r x_2 + b_2(u_3 + f_{a2}) \\
\dot{x}_5 &= x_6 \\
\dot{x}_6 &= a_7x_2x_4 + a_8x_6^2 + b_3(u_4 + f_{a3}) \\
\dot{x}_7 &= x_8 \\
\dot{x}_8 &= a_9x_8 + \frac{1}{m}u_x u_1 \\
\dot{x}_9 &= x_{10} \\
\dot{x}_{10} &= a_{10}x_{10} + \frac{1}{m}u_y u_1 \\
\dot{x}_{11} &= x_{12} \\
\dot{x}_{12} &= a_{11}x_{12} - g + \frac{C\phi C\theta}{m}(u_1 + f_{a4})
\end{aligned} \tag{30}$$

$$\begin{aligned} y = [&x_1x_2 + f_{s1}x_3x_4 + f_{s2}x_5x_6 + f_{s3} \\ &x_7x_8 + f_{s4}x_9x_{10} + f_{s5}x_{11}x_{12} + f_{s6}]^T \end{aligned} \tag{31}$$

And:

$$\begin{cases} a_1 = \frac{I_{yy} - I_{zz}}{I_{xx}}, a_2 = -\frac{K_{fax}}{I_{xx}} \\ a_3 = -\frac{J_r}{I_{xx}}, a_4 = \frac{I_{zz} - I_{xx}}{I_{yy}} \\ a_5 = -\frac{K_{fay}}{I_{yy}}, a_6 = \frac{J_r}{I_{yy}} \\ a_7 = \frac{I_{xx} - I_{yy}}{I_{zz}}, a_8 = -\frac{K_{faz}}{I_z} \\ a_9 = -\frac{K_{ftx}}{m}, a_{10} = -\frac{K_{fty}}{m} \\ a_{11} = -\frac{K_{ftz}}{m} \end{cases}, \quad \begin{cases} b_1 = \frac{l}{I_{xx}} \\ b_2 = \frac{l}{I_{yy}} \\ b_3 = \frac{l}{I_{zz}} \end{cases} \tag{32}$$

The following hypotheses are required to analyze the premise:

1- sensor faults create slow changes in time in the form of:

$$\dot{f}_{si}(t) \approx 0, i \in [1,2,3,4,5,6] \tag{33}$$

2- The resultant actuator faults are related to quadrotor movement and banked velocity sensor faults as follows:

$$|f_{ai}(t)| \le f_{ai}^{+} \;\; and \;\; |f_{sj}(t)| \le f_{sj}^{+} \;\; , i \in [1,2,3,4] \;\; and \;\; j \in \{[1,2,3,4,5,6] \tag{34}$$

Where, $\{f_{a1}^{+}, f_{a2}^{+}, f_{a3}^{+}, f_{a4}^{+}\}$ and $\{f_{s1}^{+}, f_{s2}^{+}, f_{s3}^{+}, f_{s4}^{+}, f_{s5}^{+}, f_{s6}^{+}\}$ are fixed positive amounts.

3- Unknown parts of $\gamma_{ai}(x, f_{ai}, t)$ consist of the resultants of the actuator faults related to quadrotor movements and $\gamma_{si}(x, f_{si}, t)$ related to banked velocity sensor faults as follows:

$$|\gamma_{ai}(x, f_{ai}, t)| \le |g_i(x,t)| f_{ai}^{+} < k_{ai} \;\; and \;\; |\gamma_{sj}(x, f_{sj}, t)| \le k_{sj} \quad i \in [1,2,3,4] \;\; and \;\; j \in \{[1,2,3,4,5,6] \tag{35}$$

Where, $\{k_{a1}, k_{a2}, k_{a3}, k_{a4}\}$ and $\{k_{s1}, k_{s2}, k_{s3}, k_{s4}, k_{51}, k_{s6}\}$ are fixed positive amounts.

The selected controlling strategy is based on two loops (an internal and an external loop). The internal loop entails four controlling rules: roll control, pitch control, Yaw control, and height control. The external loop entails two control rules of x and y. The external loop produces optimal amounts of roll (ϕ_d) and pitch (θ_d) through the reforming block. This block reforms roll and pitch rotations based on an optimal yaw (ψ_d). In figure 3 a summary sketch of this strategy has been represented.

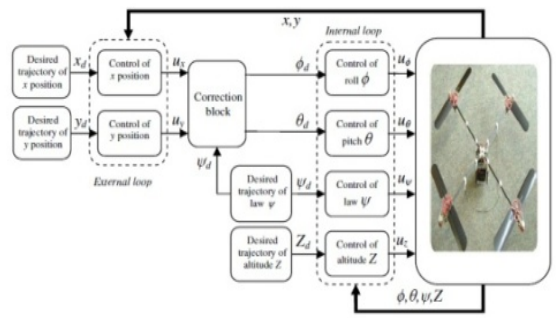

Fig.3. An integrated design of the proposed controlling strategy

Based on back-stepping model, a returning algorithm is utilized to integrate control rules that enforce the system to follow the optimal route in the presence of actuator and sensor faults:

$$e_i = \begin{cases} x_i - x_{id} & , i \in [1,3,5,7,9,11] \\ y_i - \dot{x}_{(i-1)d} + c_{(i-1)} e_{(i-1)} - \varsigma_{(i-1)} & , i \in [2,4,6,8,10,12] \end{cases}$$

And,

$$\varsigma_i = \begin{cases} k_i \int_0^t e_i d\tau & i \in [1,3,5,7,9,11] \\ k_i sign(e_i) & i \in [2,4,6,8,10,12] \end{cases}$$

Are the related Lyapanov equations as follows:

$$V_i = \begin{cases} \frac{1}{2}e_i^2 + \frac{1}{2}e_{fj}^2 & i \in [1,3,5,7,9,11], j \in [1,2,3,4,5,6] \\ V_{i-1} + \frac{1}{2}e_i^2 & i \in [2,4,6,8,10,12] \end{cases}$$

And,

$$\begin{cases} e_{fj} = f_{sj} - \varsigma_i & i \in [1,3,5,7,9,11] \text{ and } j \in [1,2,3,4,5,6] \\ \gamma_j = \begin{pmatrix} c_i & k_i \\ 1 & 0 \end{pmatrix} > 0 & i \in [1,3,5,7,9,11] \text{ and } j \in [1,2,3,4,5,6] \\ c_i > 0 & i \in [2,4,6,8,10,12] \\ k_i > \begin{Bmatrix} k_{sj} + k_{aj'} & j \in [1,2,3,6] \text{ and } j' \in [1,2,3,4] \\ k_{sj} & j \in [4,5] \end{Bmatrix} & i \in \{2,4,6,8,10,12\} \end{cases}$$

The summary of the controlling relations achieved are represented as follows:

$$\begin{cases} u_2 = \frac{1}{b_1}\begin{pmatrix} \ddot{x}_{1d} - c_1\left(-c_1e_1 + k_1\int_0^t e_1 d\tau + e_2\right) + (k_1 - 1)e_1 \\ -c_2e_2 - a_1y_4y_6 - a_2y_2^2 - a_3\bar{\Omega}_r y_4 - k_2 sign(e_2) \end{pmatrix} \\ u_3 = \frac{1}{b_2}\begin{pmatrix} \ddot{\theta}_d - c_3\left(-c_3e_3 + k_3\int_0^t e_3 d\tau + e_4\right) + (k_3 - 1)e_3 \\ -c_4e_4 - a_4y_2y_6 - a_5y_4^2 - a_6\bar{\Omega}_r y_2 - k_4 sign(e_4) \end{pmatrix} \\ u_4 = \frac{1}{b_3}\begin{pmatrix} \ddot{\psi}_d - c_5\left(-c_5e_5 + k_5\int_0^t e_5 d\tau + e_6\right) + (k_5 - 1)e_5 \\ -c_6e_6 - a_7y_2y_4 - a_8y_6^2 - k_6 sign(e_6) \end{pmatrix} \\ u_x = \frac{m}{u_1}\begin{pmatrix} \ddot{x}_d - c_7\left(-c_7e_7 + k_7\int_0^t e_7 d\tau + e_8\right) + (k_7 - 1)e_7 \\ -c_8e_8 - a_9y_8 - k_8 sign(e_8) \end{pmatrix} \quad /u_1 \neq 0 \\ u_y = \frac{m}{u_1}\begin{pmatrix} \ddot{y}_d - c_9\left(-c_9e_9 + k_9\int_0^t e_9 d\tau + e_{10}\right) + (k_9 - 1)e_9 \\ -c_{10}e_{10} - a_{10}y_{10} - k_{10} sign(e_{10}) \end{pmatrix} \quad /u_1 \neq 0 \\ u_1 = \frac{m}{Cx_1Cx_3}\begin{pmatrix} \ddot{z}_d - c_{11}\left(-c_{11}e_{11} + k_{11}\int_0^t e_{11} d\tau + e_{12}\right) + (k_{11} - 1)e_{11} \\ -c_{12}e_{12} - a_{11}y_{12} + g - k_{12} sign(e_{12}) \end{pmatrix} \end{cases}$$

Proof: for i=1, we have:

$$i = 1 \rightarrow \begin{cases} e_1 = x_1 - x_{1d} \\ V_1 = \frac{1}{2}e_1^2 + \frac{1}{2}e_{f1}^2 \end{cases}$$

$$\dot{V}_1 = e_1(\dot{x}_{1d} - c_1e_1 + \varsigma_1 - f_{s1} - \dot{x}_{1d}) + e_{f1}$$

In order to compensate the effect of roll movement velocity sensor fault, we introduce an integral that can alleviate the trace fault. We consider:

$$\varsigma_1 = k_{ks1}\int_0^t e_1\, d\tau$$

Therefore, we have:

$$\dot{V}_1 = -(e_1 \quad e_{f1})\begin{pmatrix} c_1 & 1 \\ k_1 & 0 \end{pmatrix}\begin{pmatrix} e_1 \\ e_{f1} \end{pmatrix} = -e_1^{-T}\Upsilon_1\bar{e}_1 \leq 0$$

C_1 and k_1 are utilized to make a definite positive matrix of Υ_1 and this means that $\dot{V}_1 \leq 0$.

For i=2, we have:

$$i = 2 \rightarrow \begin{cases} e_2 = y_2 - \dot{x}_{1d} + c_1e_1 - \varsigma_1 \\ V_2 = V_1 + \frac{1}{2}e_2^2 \end{cases}$$

And

$$\dot{V}_2 = e_1(-c_1e_1 - e_{f1}) + e_{f1}[(-k_1e_1) + e_2(a_1y_4y_6 + a_2y_2^2 + a_3\bar{\Omega}_r x_4 + b_1(u_2 + f_{a1}) - \ddot{x}_{1d} + c_1(-c_1e_1 - e_{f1}) - k_1 + \Upsilon a_1 + b_1u_2]$$

The consistency of (e_1, e_2) can be calculated through the introduction of a u_2 input control as follows:

$$u_2 = \frac{1}{b_1}(\ddot{x}_{1d} - c_1(-c_1e_1 + \varsigma_1 + e_2) + (k_1 - 1)e_1 - c_2e_2 - a_1y_4y_6 - a_2y_2^2 - a_3\bar{\Omega}_r y_4 - \varsigma_2), c_2 > 0$$

And,

$$\dot{V}_2 = -e_1^{-T}\Upsilon_1\bar{e}_1 - c_2e_2^2 - e_2(\varsigma_2 - \Upsilon_{a1}))$$

$$|\Upsilon a_1| = b_1|fa_1| < k_2$$

$$\varsigma_2 = k_2 sign(e_2) \rightarrow \dot{V}_2 \leq -e_1^{-T}\Upsilon_1\bar{e}_1 - c_2e_2^2 - |e_2|(k_2 - |\Upsilon_{a1}|)$$

$$(k_2 - |\Upsilon_{a1}|) > 0 \rightarrow\rightarrow \dot{V}_2 \leq 0$$

The stages above are repeated to calculate u_3, u_4, u_x, and u_y.

Simulation

Simulation is done in two forms. First without faults of the actuator and sensor and then regarding the faults in sensor and actuator. Sensor fault is considered %50 of the maximum amounts of angular and linear velocity and the resultant fault of the actuators is related to the roll, pitch, yaw, and

height movement angles regarding %20 of the maximum amounts of them in seconds 5, 9, 12, 15, 20, 24, 27, and 30 enforced on the system. The amounts required for simulation are represented in table 1 [26].

Table 1- The amounts of parameters utilized in simulations

Parameter	*Value*
m	*0.486 kg*
g	$9.806\ {}^{m}/_{s^2}$
l	*0.25 m*
b	$2.9842\times 10^{-5}\ {}^{N}/_{rad/s}$
d	$3.2320\times 10^{-7}\ {}^{N}/_{rad/s}$
J_r	$2.8385\times 10^{-7}\ kg.m^2$
$I_{(x,y,z)}$	$diag(3.8278,3.8278,7.1345)\times 10^{-3}\ kg.m^2$
$K_{fa(x,y,z)}$	$diag(5.5670,5.5670,6.3450)\times 10^{-4}\ {}^{N}/_{rad/s}$
$K_{ft(x,y,z)}$	$diag(0.0320,0.0320,0.0480)\times 10^{-4}\ {}^{N}/_{m/s}$
K_m	$4.3\times 10^{-4}\ {}^{N.m}/_{A}$
K_g	*5.6*
R_a	*0.67 ohms*

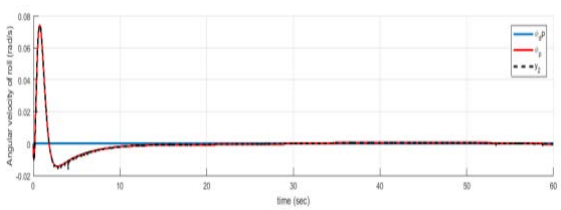

Fig.4. Angular Velocity of the Roll

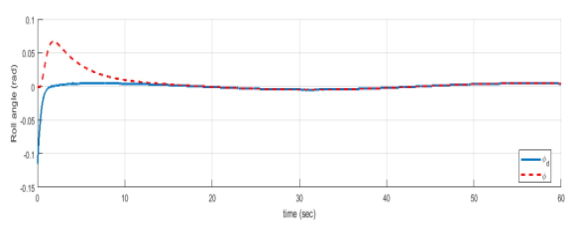

Fig.5. Angular Roll graph

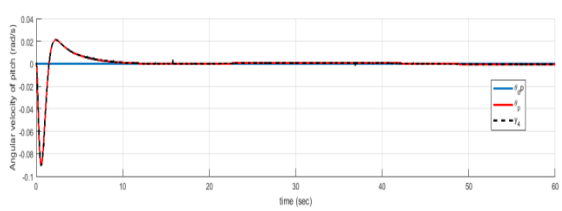

Fig.6. Angular velocity of the pitch

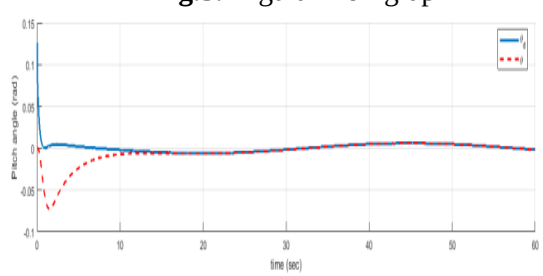

Fig.7. Pitch angle

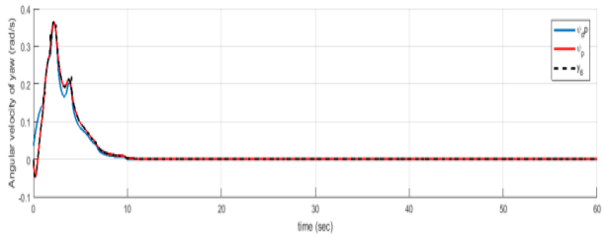

Fig.8. Angular velocity of yaw

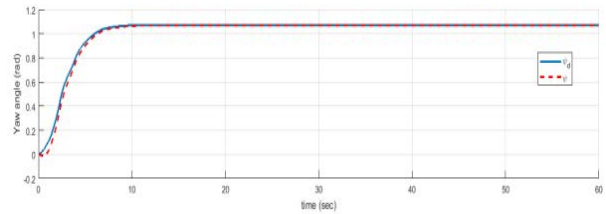

Fig.9. Yaw angle

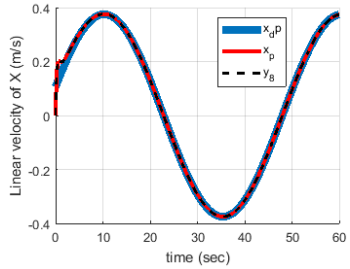

Fig.10 Linear velocity of X

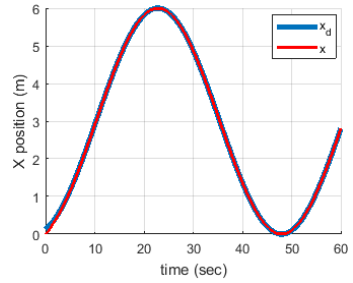

Figu.11. Movement throughout X axis

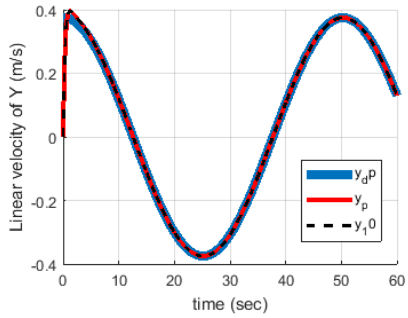

Fig.12. Linear velocity of Y

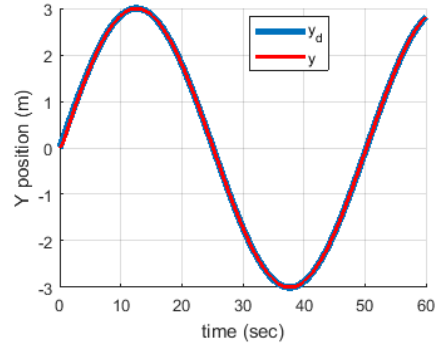

Fig.13. Movement throughout Y axis

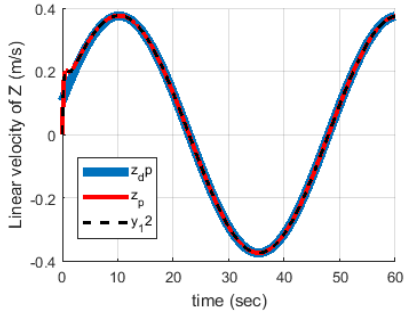

Fig.14. Linear velocity throughout X axis

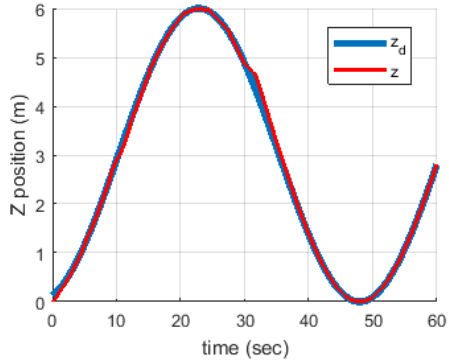

Fig.15. Movement throughout Z axis

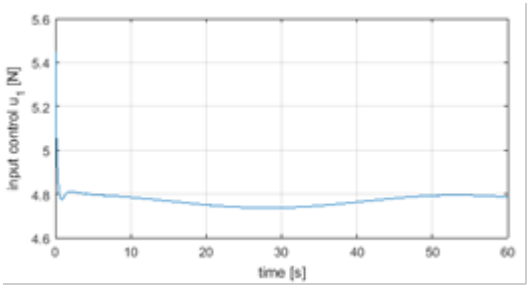

Fig.16. Input control u_1

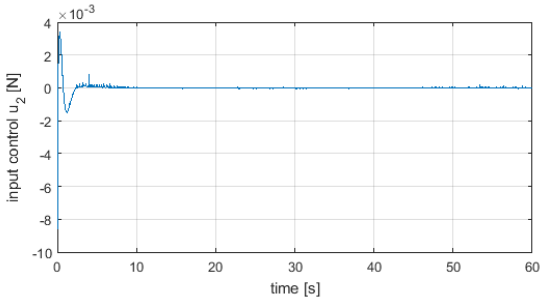

Fig.17.Input control u_2

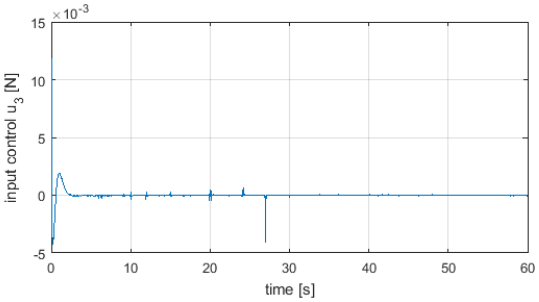

Fig.18. Input control u_3

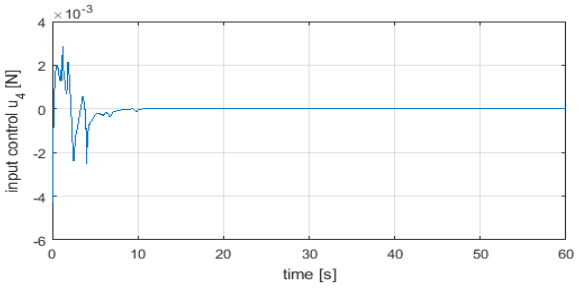

Fig.19. Input control u_4

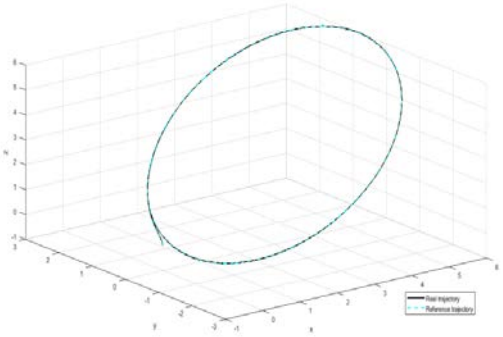

Fig.20. Flight route

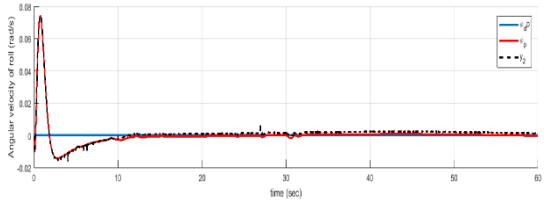

Fig.21. Angular velocity of roll

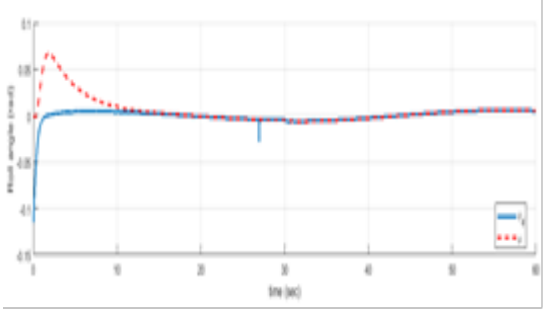

Fig.22. Roll angle

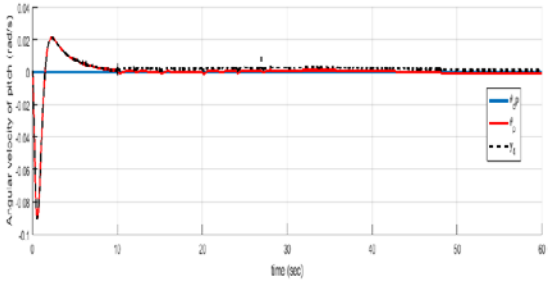

Fig.23. Angular velocity of pitch

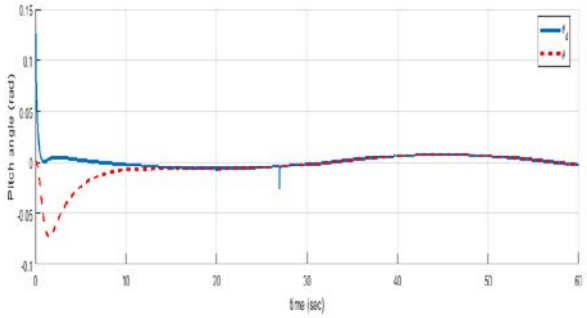

Fig.24. Pitch angle

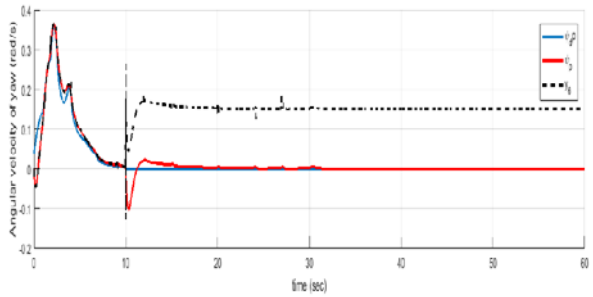

Fig.25.Angular velocity of yaw

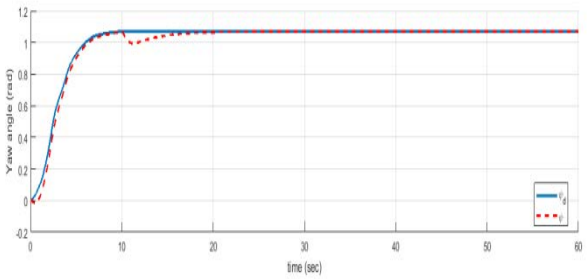

Fig.26. Yaw angle

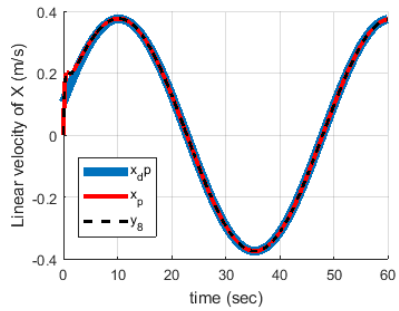

Fig.27. Linear velocity of x

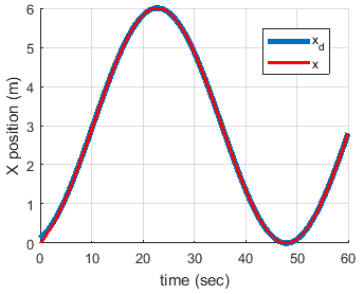

Fig.28. X position

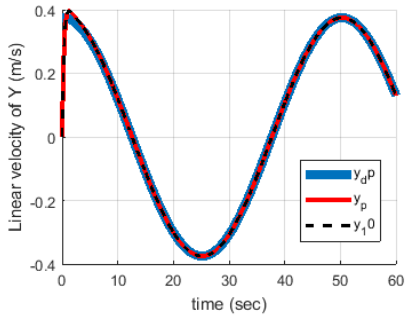

Fig. 29. Linear velocity of Y

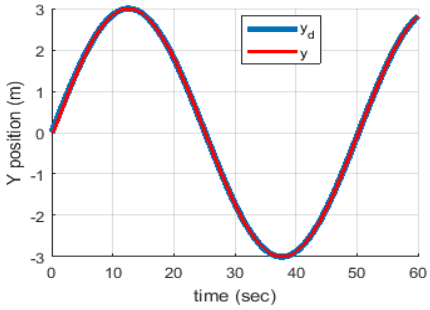

Fig.30. Y position

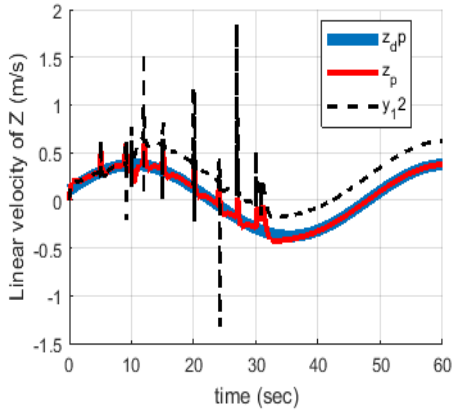

Fig.31. Linear velocity of Z

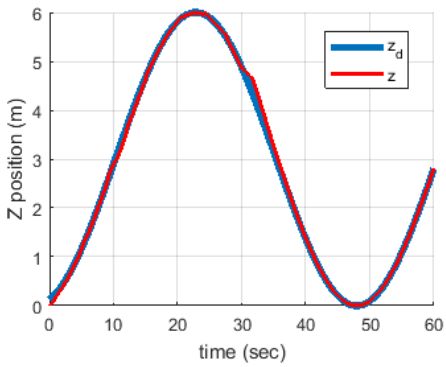

Fig.32.Z position

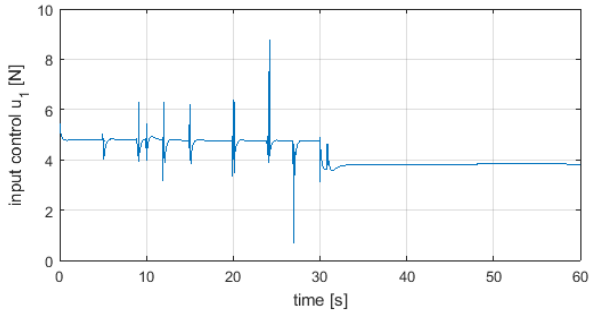

Fig.33. Input control u_1

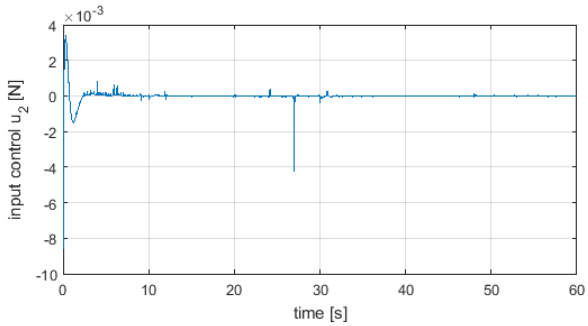

Fig.34. Input control u_2

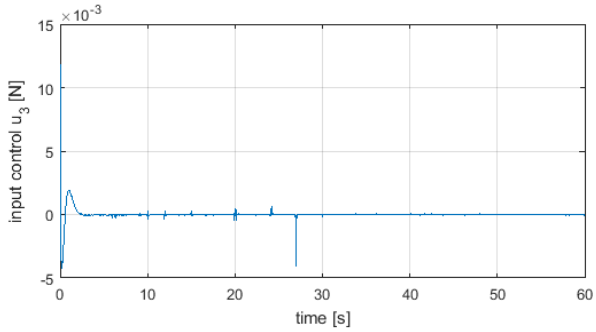

Fig.35. Input control u_3

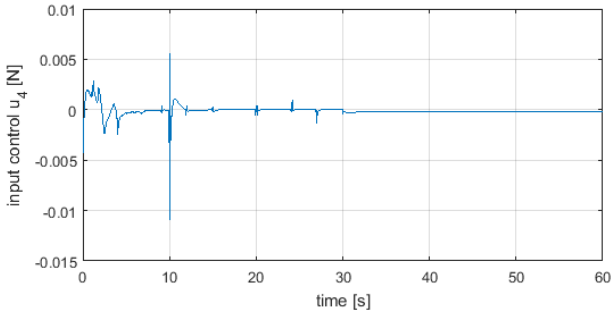

Fig.36. Input control u4

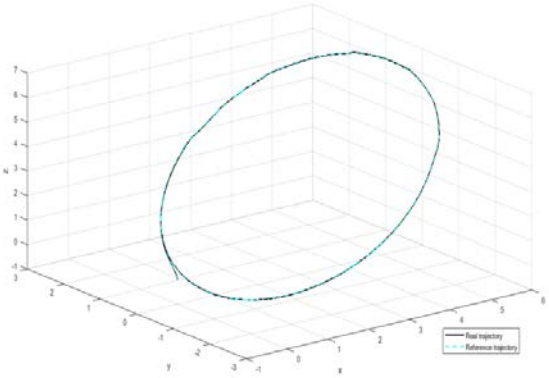

Fig.37. Flight route

In figures 4, 6, and 8 which represent angular velocity of roll, pitch, and yaw, we observed an optimal tracing. The trace of roll, pitch, and yaw angles in without fault form represented in figures 5, 7, and 9 are optimal. In without fault format, the figures of linear velocity and movement throughout the axes x, y, and z represented in figures 10, 12, 14, 11, 13, and 15 showed optimal amounts and appropriate traces. u_1, u_2, u_3, and u_4 are control signals of the system in without faults mode and are represented in figures 16, 17, 18, and 19, respectively, and they have optimal amounts, although there are some trivial fluctuations. The flight route tracing has been carried out appropriately in without fault format as it has been represented in figure 20. In the state of faults and in the presence of actuator and sensor faults enforced, the tracing of angular velocity and roll, pitch, and yaw angles represented in figures 21, 23, 25, 22, 24, and 26, respectively, has been appropriate. Figures 27, 28, 29, 30, 31, and 32 which represented linear velocity and movement throughout the axes x, y, and z in with fault format have shown appropriate tracing. In faulty format, the system control signals of u_1, u_2, u_3, and u_4 which have been represented in figures 33, 34, 35, and 36, respectively, showed optimal amounts. The flight route tracing has been carried out appropriately in faulty format as it has been represented in figure 37.

Results and discussion

In the present study first we have used Newton-Euler method to model the quadrotor. Then, the resistant control based on back-stepping has been utilized to control the system. Actuator and sensor faults were added to the system afterwards. Then, the control rules were calculated for a state through which the system encountered with faults in the actuator and the sensor. The system consistency was approved using Lyapanov functions. The simulations were carried out in MATLAB software and the results showed system consistency and efficient system control in both states (with and without faults)

References

[1] Alexis, K. Nikolakopoulos, G., Tzes, A. and Dritsas, A. Coordination of helicopter UAVs for aerial forest-fire surveillance. 44 IEEE Conf. ‘Application of intelligent control Decision and Control, 2005 European Control of engineering systems’ Springer, The Netherlands, pp 169-193, 2009.

[2] Barghandan, S., Badamchizadeh, M.A. and Jahed-Motlagh, M.R. Improved Adaptive Fuzzy Sliding Mode Controller for Robust Fault Tolerant of a Quadrotor. International Journal of Control, Automation and Systems, 15(X) pp. 1-15, 2017.

[3] Boabdollah, S., Muurrieri, P. and Seigwart, R. Design and control of indoor micro quadrotor. IEEE International Conf. on Robotics and Automation, New Orleans, pp. 4393-4400, 2002.

[4] Borji-Monfared, Sadra; Kalhor, Ahmad; Amiri Atashgah, Mohammadali, Resistant nonlinear control of H_∞ and predicator of quadrotor route tracing using system parameters estimation. Journal of Mechanical Engineering in Modarres University, 2016, (7), 32-42.

[5] Bouabdallah, S. and Siegwart, R. Back-stepping and Sliding-mode Techniques Applied to an Indoor Micro Quadrotor. Proceedings of the 2005 IEEE International Conference on Robotics and Automation, Barcelona, Spain, April 2005.

[6] Capari, G., Breitenmoser, A. and Fisher, W. et al. Highly compact robots for inspection of power plants. Journal of Field Robotics., 29, (1), pp 47-68, 2012.

[7] Colorado, J. Barrientos, A. Martinez, A. Lafaverges, B. and Valente, J. Mini-quadrotor Attitude Control based on Hybrid Back-stepping & Frenet-Serret Theory. 2010 IEEE International Conference on Robotics and Automation Anchorage Convention District, May 3-8, 2010, Anchorage, Alaska, USA.

[8] Committee on Autonomous in Support of Naval Operation, National Research Council. Autonomous vehicle in support of naval operations. Naval studies Board, Washington DC, USA, 2005.

[9] Ghasemi, Kobra, Designing a nonlinear controller for the quadrotor. M.SC. dissertation, Tabriz University, 2011.

[10] Girad, A., Howell, A. and Hedrick, J. Border patrol and surveillance mission using multiple unmanned air vehicle. 43rd IEEE Conf. on Decision and Control, Atlantis, Paradise , Islands, Bahamas, December , vol. 1, pp 620-625, 2004.

[11] Herwits, S.R., Johnson, L.F. and Dnagan, S.E. et al. W. Imaging from an unmanned aerial vehicle: agricultural and decision support. Computer Electronic Agriculture, 44, (1), pp 49-61, 2004.

[12] Hoffman, G.M., Huang, H., Waslander, S.L. and Tomlin, C.J. Quadrotor helicopter dynamics and control: theory and Experiment. Proc. Guidance, Navigation and Control Conf., 2007.

[13] Hovakimyan, N. et al. Adaptive output feedback control of uncertain nonlinear systems using single-hidden- layer neural networks. IEEE. Trans. On Neural Networks, vol. 13, pp. 1420-1431, 2002.

[14] Huang, M., Xian, B. Diao, C. Yang, K. and Feng, Y. Adaptive Tracking Control of Under-actuated Quadrotor Unmanned Aerial Vehicles via Back-stepping. 2010 American Control Conference Marriott Waterfront, Baltimore, MD, USA ,June 30-July 02, 2010.

[15] Khebbache, H. Sait, B. Bounar, N. and Yacef, F. ROBUST STABILIZATION OF A QUADROTOR UAV IN PRESENCE OF SENSOR FAULTS. International Journal of Instrumentation and Control Systems (IJICS) Vol.2, No.2, April 2012.

[16] Miguel Brito Domingues, J. Quadrotor prototype. Engenharia Mecanica. October 2009.

[17] Mokhtari, A., Benallegue, A, and Daachi, B. Robot feedback linearization and GH infinity controller for a quadrotor unmanned aerial vehicle .Journal of Electrical Engineering, 57(1), pp. 20-27, 2006.

[18] Murphy, D. and Cycon, J. Applications for mini VTOL UAV for law enforcement. Information and Training Technology for Law Enforcement, Boston ,MA, USA, November,1998.

[19] Nicol, C.Macnab, C.J.B. and Ramirez-Serrano, A. ROBUST NEURAL NETWORK CONTROL OF A QUADROTOR HELICOPTER. Electrical and Computer Engineering, 2008, CCECE 2008. Canadian Conference on Electrical and Computer Engineering, Niagara Falls, Canada, May 2008.

[20] Pounds, P., Mahony, R., Gresham, J., Croke, P., and Roberts, J. Toward. Dynamically- Favorable Quad-Rotor Aerial Robots. Proceedings of the 2004 Australasian Conference on Robotics & Automation, Australian Robotics & Automation Association, Australian National University Canberra.

[21] Qian, M.S. Jiang, B. and Liu, H.H.T. Dynamic Surface Active Fault Tolerant Control Design for the Attitude Control Systems of UAV with Actuator Fault. International Journal of Control, Automation and Systems, 14(3),pp. 723-732, 2016.

[22] Ryan, A. and Hedrich, A. A mode-switching path planner for UAV-assisted search and rescue. 44 IEEE Conf. Decision and Control, 2005 European Control Conf. CDC-ECC 05, Seville, Spain, pp. 1471-1476, 2005.

[23] Tayebi, A. and McGilvary, S. Atltituude stabilization of a four rotor robot. 43rd IEEE Conference on Decision and control, Bahamas, 2004.

[24] Wang, B. and Zhang, Y. Fuzzy Adaptive Fault-Tolerant Control for Quadrotor Helicopter .2017 International Conference on Unmanned Aircraft Systems (ICUAS), June 13-16, 2017, Miami, FL, USA.

[25] Yang, H. Jiang, B. and Zhang, K. Direct Self-repairing Control of the Quadrotor Helicopter Based on Adaptive Sliding Mode Control Technique. Proceedings of 2014 IEEE Chinese Guidance, Navigation and Control Conference August 8-10, 2014, Yantai, China.

[26] Zhaohui Cen, Zh. Hassan Noura, H. Susilo, T.B. and Al Younes. Y. Robust Fault Diagnosis for Quadrotor UAVs Using Adaptive Thau Observer. Springer, 2013.